Inhibition of Linear Absorption in Opaque Materials Using Phase-Locked Harmonic Generation

Marco Centini,[1] Vito Roppo,[2,4] Eugenio Fazio,[1] Federico Pettazzi,[1] Concita Sibilia,[1] Joseph W. Haus,[3] John V. Foreman,[4,5] Neset Akozbek,[4] Mark J. Bloemer,[4] and Michael Scalora[4]

[1]*Dipartimento di Energetica, University of Rome La Sapienza, Via Scarpa 16, Rome, Italy*
[2]*Departament de Fisica i Enginyeria Nuclear, Universitat Politecnica de Catalunya C/Colom 11, 08222 Terrassa, Spain*
[3]*Electro-Optics Program, University of Dayton, Dayton, Ohio 45469-0245, USA*
[4]*Charles M. Bowden Research Facility, RDECOM, U.S. Army Aviation and Missile Command, Redstone Arsenal, Alabama 35803, USA*
[5]*Department of Physics, Duke University, Durham, North Carolina 27708, USA*

(Received 17 April 2008; revised manuscript received 24 July 2008; published 11 September 2008)

We theoretically predict and experimentally demonstrate inhibition of linear absorption for phase and group velocity mismatched second- and third-harmonic generation in strongly absorbing materials, GaAs, in particular, at frequencies above the absorption edge. A 100-fs pump pulse tuned to 1300 nm generates 650 and 435 nm second- and third-harmonic pulses that propagate across a 450-μm-thick GaAs substrate without being absorbed. We attribute this to a phase-locking mechanism that causes the pump to trap the harmonics and to impress on them its dispersive properties.

DOI: 10.1103/PhysRevLett.101.113905 PACS numbers: 42.25.Bs, 42.65.Ky

Since its inception in the early 1960s, the study of nonlinear frequency conversion has focused on improving the efficiency of the process in transparent materials [1–6]. Nonlinear conversion rates depend on factors such as phase and group velocity mismatch and peak pump intensity. Linear absorption is considered detrimental since it is assumed that the generated harmonics are reabsorbed. Harmonic generation in absorbing materials and/or semiconductors at frequencies above the absorption edge has been considered in the context of measuring the nonlinear coefficients [7–13], but it has not been as widely studied as in the transparency range. For example, the enhancement of third-harmonic generation in various types of glasses opaque to third-harmonic (TH) light was experimentally demonstrated [11]. UV second-harmonic generation (SHG) above the absorption band edge in $LiNbO_3$ [12] as well as UV and x-ray [13] SHG in semiconductors have been reported. These examples show that the subject is of interest for the purpose of realizing coherent sources and because of the many potential applications that semiconductors find in optical technology.

A better understanding of propagation phenomena at or above the absorption edge of semiconductor and dielectric materials [14] is needed not only in view of the discrepancies that exist between predictions and experimental observations [11,12] but also because in this range semiconductors such as GaAs display a negative dielectric permittivity. This raises the possibility of new effects related to negative refraction of light at optical and UV wavelengths, absorption notwithstanding. A systematic examination of dynamics and nonlinear frequency conversion above the absorption edge of semiconductors is still lacking primarily because these processes are thought to be uninteresting and inefficient, due to absorption and the naturally high degree of phase mismatch. In this Letter, we dispel this notion and predict and experimentally observe the inhibition of absorption for femtosecond, SH and TH (650 and 435 nm, respectively) signals in a GaAs substrate 450 microns thick. In the opaque region, the characteristic absorption lengths of GaAs are much less than 1 μm: Linear transmittance through a one-micron-thick GaAs substrate is $\sim 10^{-4}$ at 532 nm and $\sim 10^{-8}$ at 364 nm.

Bulk GaAs becomes opaque below ~900 nm. Our theory shows that the pump, tuned to a region of optical transparency, captures and impresses its dispersive properties on portions of the generated harmonic signals, which in turn behave as parts of the pump and copropagate for the entire length of the sample without being absorbed. This spectacular behavior is brought about by a phase-locking phenomenon [15] that impacts harmonic generation and other types of parametric processes, with seeded or unseeded harmonic signals. These general conclusions apply: If the medium is transparent at the pump frequency, then the material will be transparent at the harmonic frequencies. Similarly, if the medium absorbs the pump and is transparent in the SH and TH ranges, the phase-locked components are absorbed.

The prediction of a two-component SH signal (homogenous and inhomogeneous solutions of the wave equation) was made early on [4] and was later discussed and observed [5,6]. In transparent materials, the pulsed SHG process develops as follows: The inhomogeneous signal is trapped by the pump and propagates at the pump's group velocity [15]. The homogeneous component propagates according to material dispersion and eventually walks off from the pump. In absorbing materials [7–13], Maker fringes [3] are observed as long as material absorption is small, while the amplitude of the transmitted beam is independent of sample thickness [12]. Thus, the evidence

suggests that Maker fringes disappear when the interaction between the pump and the homogenous SH component stops. This can occur if the homogenous component either is absorbed or walks off from the pump, in both cases leaving the phase-locked signals intact. Even though these predictions and observations are not new, it was not until recently that in transparent materials these phenomena were cast in terms of a phase-locking mechanism [15] that also impacts higher order nonlinearities [16]. Calculations show that the trapped signals acquire the dispersive properties of the pump; i.e., they propagate with the pump's index and group velocity. If the group velocity mismatch is relatively large, the pump and the homogenous SH components separate immediately upon entering the medium, and the conversion process turns into a surface phenomenon: The pump field and its captive harmonic signals do not exchange energy inside the medium [15]; i.e., their relative phase difference is constant, until another interface is crossed.

In absorbing materials, discrepancies have been recorded between predictions and experimental results [11,12]. Even though there is recognition that the two generated SH components propagate at different group velocities and have peculiar phase properties [17], a spectral analysis reveals a far more intimate connection than previously thought between the pump and the trapped harmonic pulses, i.e., a phase locking that binds the pulses spatially and temporally [15]. In the present analysis, we calculate the energy velocities of the generated pulses, defined as usual: $V_e = \frac{\langle S \rangle}{\langle U \rangle}$, where $S = \frac{c}{4\pi}\mathbf{E} \times \mathbf{H}$ is the Poynting vector and U the energy density; the brackets mean a definite integral. The group velocity calculated as $V_g = \frac{\partial \omega}{\partial k}$ is not adequate, because this value describes the homogenous signal. Experimental and theoretical evidence [5,6,15] show that the pump and the phase-locked pulses propagate at the same energy velocity. In confirmation of the fact that the generated fields behave in all respects as if they were pump fields, our calculations show that the proper energy velocities for the second- and third-harmonic fields (that is to say, the velocity of the pump field) are recovered only if the Landau energies [18] $U(z,t) = \frac{1}{8\pi}[\mathrm{Re}(\frac{\partial[\omega\varepsilon(\omega)]}{\partial\omega})|\mathbf{E}|^2 + \mathrm{Re}(\frac{\partial[\omega\mu(\omega)]}{\partial\omega})|\mathbf{H}|^2]$ are evaluated with the material parameters of the pump frequency. Therefore, we find that V_e is identical for all pulses only if the generated harmonic fields are attributed the material dispersion of the pump. This finding cements the notion that the phase-locked pulses behave as the pump pulse does and ultimately are required to be treated as such in the application of boundary conditions.

To model simultaneous second- and third-harmonic generation in ordinary materials, we assume that the fields may be decomposed as a superposition of harmonics:

$$\begin{aligned}\mathbf{E} &= \hat{\mathbf{x}}\sum_{\ell=1}^{\infty}[E_{\ell\omega}(z,t) + \text{c.c.}] = \hat{\mathbf{x}}\sum_{\ell=1}^{\infty}[\mathcal{E}_{\ell\omega}(z,t)e^{i\ell(kz-\omega t)} + \text{c.c.}],\\ \mathbf{H} &= \hat{\mathbf{y}}\sum_{\ell=1}^{\infty}[H_{\ell\omega}(z,t) + \text{c.c.}] = \hat{\mathbf{y}}\sum_{\ell=1}^{\infty}[\mathcal{H}_{\ell\omega}(z,t)e^{i\ell(kz-\omega t)} + \text{c.c.}],\end{aligned} \tag{1}$$

where $\mathcal{E}_{\ell\omega}$ and $\mathcal{H}_{\ell\omega}$ are generic, spatially and temporally dependent, complex envelope functions; k and ω are the carrier wave vector and frequency, respectively, and ℓ is an integer. Equations (1) are a convenient representation of the fields, and no *a priori* assumptions are made about the envelopes. The linear response of the medium is described by a Lorentz oscillator model: $\varepsilon(\omega) = 1 - \frac{\omega_p^2}{\omega^2 + i\gamma\omega - \omega_r^2}$, and $\mu(\omega) = 1$, where γ, ω_p, and ω_r are the damping coefficient and the plasma and resonant frequencies, respectively. Second- and third-order nonlinearities are introduced as a nonlinear polarization of the type: $P_{\mathrm{NL}} = \chi^{(2)}E^2 + \chi^{(3)}E^3$. Assuming that the polarization and currents may be decomposed as in Eqs. (1), and that no diffraction is present, we obtain the following Maxwell-Lorentz system of equations for the lth field components:

$$\begin{aligned}&\frac{\partial\mathcal{E}_{\ell\omega}}{\partial\tau} = i\beta_{\ell\omega}(\mathcal{E}_{\ell\omega} - \mathcal{H}_{\ell\omega}) - 4\pi(\mathcal{J}_{\ell\omega}\mathcal{P}_{\ell\omega}) - \frac{\partial\mathcal{H}_{\ell\omega}}{\partial\xi} + i4\pi\beta_{\ell\omega}\mathcal{P}^{\mathrm{NL}}_{\ell\omega} - 4\pi\frac{\partial\mathcal{P}^{\mathrm{NL}}_{\ell\omega}}{\partial\tau}, \quad \frac{\partial\mathcal{H}_{\ell\omega}}{\partial\tau} = i\beta_{\ell\omega}(\mathcal{H}_{\ell\omega} - \mathcal{E}_{\ell\omega}) - \frac{\partial\mathcal{E}_{\ell\omega}}{\partial\xi},\\ &\frac{\partial\mathcal{J}_{\ell\omega}}{\partial\tau} = (2i\beta_{\ell\omega} - \gamma_{\ell\omega})\mathcal{J}_{\ell\omega} + (\beta_{\ell\omega}^2 + i\gamma\beta_{\ell\omega} - \beta_{r,\ell\omega}^2)\mathcal{P}_{\ell\omega} + \pi\omega_{p,\ell\omega}^2\mathcal{E}_{\ell\omega}, \quad \frac{\partial\mathcal{P}_{\ell\omega}}{\partial\tau} = \mathcal{J}_{\ell\omega},\end{aligned} \tag{2}$$

where $\mathcal{J}_{\ell\omega'}$ $\mathcal{P}_{\ell\omega'}$ and $\mathcal{P}^{\mathrm{NL}}_{\ell\omega}$ are the linear current and the linear and nonlinear polarizations, respectively. The coordinates are scaled so that $\xi = z/\lambda_0$, $\tau = ct/\lambda_0$, $\omega_0 = \frac{2\pi c}{\lambda_0}$, where $\lambda_0 = 1$ μm is a convenient reference wavelength; $\gamma_{\ell\omega}$, $\beta_{\ell\omega} = 2\pi\ell\omega/\omega_0$, $\beta_{r,\ell\omega} = 2\pi\omega_{r,\ell\omega}/\omega_0$, and $\omega_{p,\ell\omega}$ are the scaled damping coefficient, wave vector, and resonance and plasma frequencies for the ℓth harmonic, respectively. Expanding the field powers in terms of generic envelope functions leads to

$$\begin{aligned}\mathcal{P}^{\mathrm{NL}}_{\omega} &= 2\chi^{(2)}(\mathcal{E}^*_{2\omega}\mathcal{E}_{3\omega} + \mathcal{E}^*_{\omega}\mathcal{E}_{2\omega}) + 3\chi^{(3)}(|\mathcal{E}_{\omega}|^2\mathcal{E}_{\omega} + \mathcal{E}^2_{2\omega}\mathcal{E}^*_{3\omega} + \mathcal{E}_{3\omega}\mathcal{E}^{*2}_{\omega} + 2|\mathcal{E}_{2\omega}|^2\mathcal{E}_{\omega} + 2|\mathcal{E}_{3\omega}|^2\mathcal{E}_{\omega}),\\ \mathcal{P}^{\mathrm{NL}}_{2\omega} &= \chi^{(2)}(\mathcal{E}^2_{\omega} + 2\mathcal{E}^*_{\omega}\mathcal{E}_{3\omega}) + 3\chi^{(3)}(|\mathcal{E}_{2\omega}|^2\mathcal{E}_{2\omega} + 2|\mathcal{E}_{3\omega}|^2\mathcal{E}_{2\omega} + 2\mathcal{E}^*_{2\omega}\mathcal{E}_{3\omega}\mathcal{E}_{\omega} + 2|\mathcal{E}_{\omega}|^2\mathcal{E}_{2\omega}),\\ \mathcal{P}^{\mathrm{NL}}_{3\omega} &= 2\chi^{(2)}\mathcal{E}_{2\omega}\mathcal{E}_{\omega} + \chi^{(3)}(\mathcal{E}^3_{\omega} + 6|\mathcal{E}_{2\omega}|^2\mathcal{E}_{3\omega} + 3|\mathcal{E}_{3\omega}|^2\mathcal{E}_{3\omega} + 3\mathcal{E}^2_{2\omega}\mathcal{E}^*_{\omega} + 6|\mathcal{E}_{\omega}|^2\mathcal{E}_{3\omega}).\end{aligned} \tag{3}$$

Equations (2) represent 12 nonlinear coupled equations supplemented by Eqs. (3) and are solved using a time-domain,

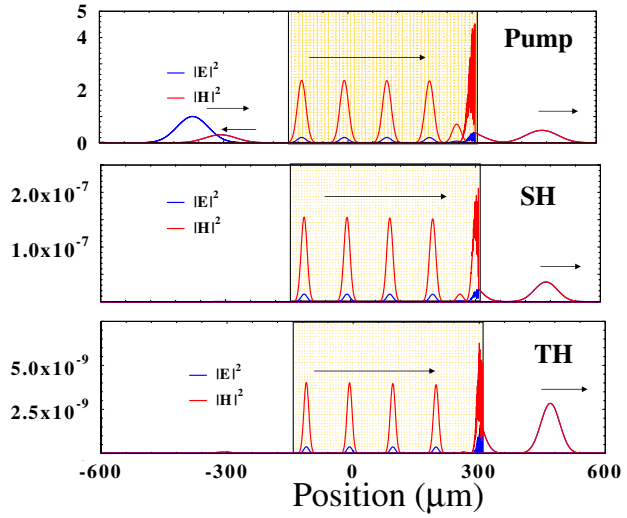

FIG. 1 (color online). Pump and harmonic pulses propagating through a GaAs substrate. The Lorentz parameters are $\omega_p = 9.425$, $\omega_r = 2.98$, and $\gamma = 0$ ($n \sim 3.41$) for the pump ($\gamma = 0$ effectively makes the medium transparent to the pump); $\omega_p = 9.425$, $\omega_r = 2.98$, and $\gamma = 0.5$ ($n = 3.83 + i0.18$) for the SH; and $\omega_p = 9.425$, $\omega_r = 2.98$, and $\gamma = 1.65$ ($n = 4.65 + i1.25$) for the TH. Only the phase-locked components survive.

split-step, fast Fourier transform-based pulse propagation algorithm [19]. Solving Eqs. (2) without introducing absorption reveals the existence of trapped and homogeneous SH and TH components. The homogeneous components generally travel at group velocities slower than the pump and eventually walk off. The pump and the trapped portions of the SH and TH signals travel at the same energy velocity. The generation of the homogeneous and phase-locked components is thus a fundamental property of the nonlinear process, independent of material parameters, and is discussed in detail in Ref. [15].

What happens when significant absorption is present at the harmonic frequencies? We simulate the propagation of 100-fs, 160 MW/cm^2 incident pulses inside a 450-micron-thick GaAs substrate tuned to 1300 nm. The peak power used avoids shape changes due to self- and cross-phase modulation and nonlinear pump absorption, which under these conditions could impact the dynamics if the sample were several millimeters thick. For short-enough incident pulses, linear dispersion can steadily erode the peak intensity of the pump pulse, a process that mimics pump depletion and reduces the coupling to the harmonic fields inducing their decay. With these considerations in mind, in Fig. 1, we show the pump and the trapped harmonic pulses propagating through a GaAs substrate. In Fig. 2, we depict the power spectrum of the pulses shown in Fig. 1. These profiles become stationary once the pump is completely inside the substrate. In Figs. 1 and 2, we note the absence of the homogeneous components; their spectral positions are marked by vertical red (SH) and blue (TH) lines in Fig. 2. In Fig. 3, we show the energies of the pump and harmonic pulses inside and to the right of the substrate.

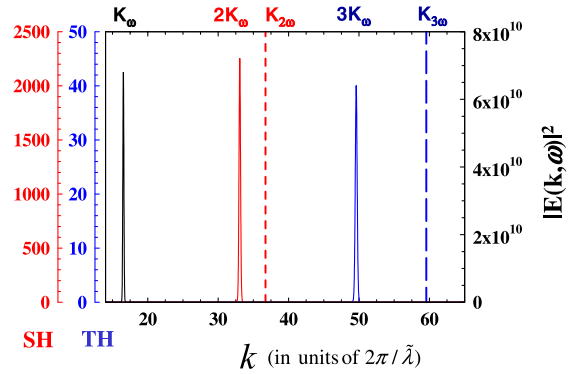

FIG. 2 (color online). k-space spectrum of the fields depicted in Fig. 1. The vertical, dashed lines show the position of the homogeneous components had absorption been neglected.

From this figure, one discerns that the SH and TH energies are generated at the entry surface and remain constant while the pulses transit through the sample. A spectral analysis of the signals shows that the frequency makeup of each pulse does not change with distance, an indication that no energy is exchanged. However, the pulses interact once again at the exit surface, where harmonic energy may be created (TH) and lost (SH) [15]. The top of Fig. 3 contains a plot of the complex index of refraction of GaAs, as reported by Palik [14]; the Lorentz parameters are thus chosen (see caption of Fig. 1) to reflect these data. Our calculations thus prove that the introduction of absorption causes the trapped harmonics to survive in the form of phase-locked pulses.

The predicted survival of the phase-locked SH and TH fields was experimentally verified using the setup shown in Fig. 4. An optical parametric amplifier pumped by ~100 fs, amplified Ti:sapphire pulses generated the pump at 1300 nm with a 1 kHz repetition rate. The colli-

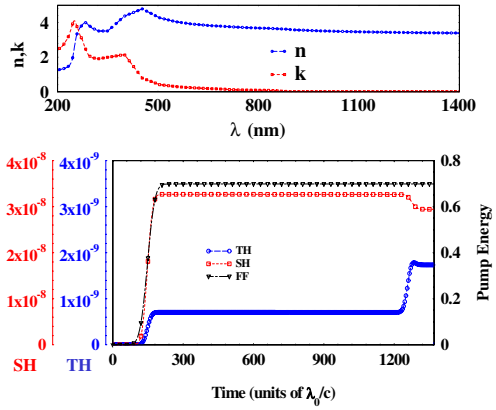

FIG. 3 (color online). Bottom: Pump (right axis) and harmonic (left axes) energies inside and to the right of the substrate. Harmonic generation occurs at entry (time ~150) and exit (time ~1200) surfaces, and the energies remain constant inside the substrate. At the exit surface, some SH energy is lost, while the TH signal nearly doubles in magnitude, although opposite behavior is also possible [15] using slightly different material dispersion.

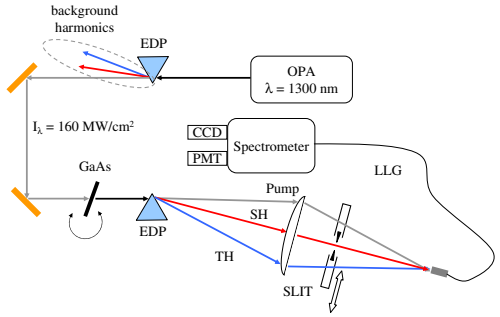

FIG. 4 (color online). Experimental setup. A beam generated by an optical parametric amplifier (OPA) irradiates a GaAs substrate. After passing through the sample, a prism [equilateral dispersing prism (EDP)] separates the harmonics. The three beams are coupled to a spectrometer via a liquid light guide (LLG) and measured using a near infrared photomultiplier tube (PMT) (for the pump) or a CCD (for the SH and TH). A moveable slit assembly provides spatial filtering so that only one beam reaches the LLG.

mated pump irradiated the GaAs substrate at an angle of 20°. This angle gave the best SH conversion efficiency; THG was less sensitive to the incident angle. After passing through the GaAs, the SH and TH fields were separated from the pump using a prism and lens/slit assembly. The signals were coupled to a spectrometer by means of a liquid light guide and were then measured using a near infrared photomultiplier tube (for the pump) or liquid nitrogen cooled CCD array (for SH and TH). The measured spectra for the pump and its first two harmonics are shown in Fig. 5. Absolute values of the SH and TH energies were calibrated by sending laser beams of known power along the same optical paths and through the same detection system, and we were able to estimate the SH and TH conversion efficiencies to be 1.3×10^{-8} and 2.5×10^{-9}, respectively. Removing the GaAs sample from the beam path caused the conversion efficiencies to drop by a factor of 20 for the SH and by a factor of 2 for the TH. Without the sample in the beam path, nearly all optical elements (metallic mirrors, prisms, etc.) yielded some SHG, while

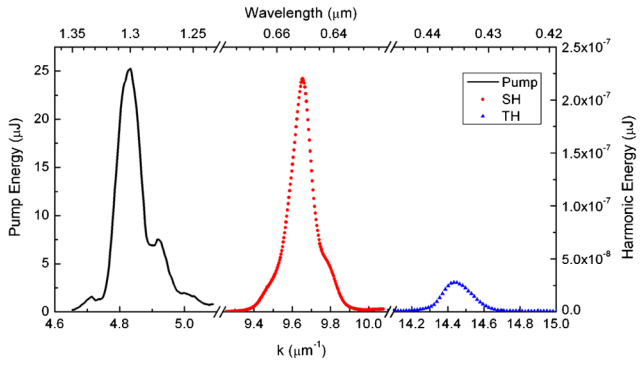

FIG. 5 (color online). Measured spectra of the pump and the transmitted harmonics. The area under each spectrum corresponds to the measured energy (2.9 μJ for pump, 3.7×10^{-8} μJ for SH, and 7.3×10^{-9} μJ for TH).

some TH signal was generated by the mere traversal of air. Conversion efficiencies and pump transmittance data were used in the model to estimate $\chi^{(2)} \sim 100$ pm/V and $n_2 \sim 10^{-11}$ cm^2/W, respectively.

In conclusion, we have presented theoretical and experimental evidence that absorption can be inhibited in opaque materials, well above the absorption edge of semiconductors and dielectrics alike. This dramatic result is due to a phase-locking mechanism that causes the pump to trap and impress its dispersive properties to the generated harmonic signals. We have shown that a GaAs substrate 450 microns thick supports the propagation of red and violet light. Our results suggest that it is possible to achieve significant nonlinear frequency conversion at high frequencies, particularly towards the UV, using readily available sources and materials and that the still relatively low conversion efficiencies can be improved significantly in a cavity environment, where phase locking still holds. Finally, as pointed out in Ref. [20], accessing regimes that are outside the norm highlights the fact that our "understanding of nonlinear wave conversion phenomena is still far from complete," with many more surprises that are likely waiting to be revealed.

[1] P. A. Franken *et al.*, Phys. Rev. Lett. **7**, 118 (1961).
[2] J. A. Giordmaine, Phys. Rev. Lett. **8**, 19 (1962).
[3] P. D. Maker *et al.*, Phys. Rev. Lett. **8**, 21 (1962).
[4] J. A. Armstrong *et al.*, Phys. Rev. **127**, 1918 (1962); N. Bloembergen and P. S. Pershan, Phys. Rev. **128**, 606 (1962).
[5] S. L. Shapiro, Appl. Phys. Lett. **13**, 19 (1968); W. H. Glenn, IEEE J. Quantum Electron. **5**, 284 (1969); J. T. Manassah and O. R. Cockings, Opt. Lett. **12**, 1005 (1987).
[6] L. D. Noordam *et al.*, Opt. Lett. **15**, 1464 (1990); R. M. Rassoul *et al.*, Opt. Lett. **22**, 268 (1997); W. Su *et al.*, J. Opt. Soc. Am. B **23**, 51 (2006).
[7] R. K. Chang, J. Ducuing, and N. Bloembergen, Phys. Rev. Lett. **15**, 415 (1965).
[8] W. K. Burns and N. Bloembergen, Phys. Rev. B **4**, 3437 (1971).
[9] E. Bringuier *et al.*, Phys. Rev. B **49**, 16 971 (1994).
[10] M. Martinelli, L. Gomes, and R. J. Horowicz, Appl. Opt. **39**, 6193 (2000).
[11] G. Veres *et al.*, Appl. Phys. Lett. **81**, 3714 (2002).
[12] J. Rams and J. M. Cabrera, J. Mod. Opt. **47**, 1659 (2000).
[13] T. J. Chen, R. N. Zitter, and R. Tao, Phys. Rev. A **51**, 706 (1995).
[14] E. D. Palik, *Handbook of Optical Constants of Solids* (Academic, New York, 1985).
[15] V. Roppo *et al.*, Phys. Rev. A **76**, 033829 (2007).
[16] N. Aközbek *et al.*, Phys. Rev. Lett. **89**, 143901 (2002).
[17] T. B. Kristensen and K. Pedersen, Opt. Commun. **233**, 219 (2004).
[18] L. D. Landau and E. M. Lifshitz, *Electrodynamics of Continuous Media* (Pergamon, New York, 1960), pp. 253–256.
[19] M. Scalora and M. E. Crenshaw, Opt. Commun. **108**, 191 (1994).
[20] N. N. Zinov'ev *et al.*, Phys. Rev. B **76**, 235114 (2007).